Simultaneous removal of cationic methylene blue and anionic reactive red 198 dyes using magnetic activated carbon nanoparticles: equilibrium, and kinetics analysis

Samer Abuzerr, Maher Darwish and Amir Hossein Mahvi

ABSTRACT

For the simultaneous adsorption of cationic dye (methylene blue, MB) and anionic dye (reactive red 198, RR198) from aqueous solution, magnetic activated carbon (MAC) nanocomposite as a promising adsorbent was prepared and used. The concentration of MB at different time intervals was determined using a UV-Vis spectrophotometer while the concentration of RR198 was determined using a high performance liquid chromatography (HPLC) system. The effect of solution pH, contact time, adsorbent amount, and dye concentration were investigated. Also, both kinetic and isotherm experiments were studied. The optimum pH was 10 and 5.5 for adsorption of MB and RR198, respectively, and the equilibrium status was achieved after 120 min. The adsorption kinetics was controlled by the pseudo-second order kinetic model more than pseudo-first order. The best-fitted isotherms were Freundlich and Langmuir models for MB and RR198, respectively. The higher values of Freundlich adsorption capacity (K_f) for MB in comparison with RR198 refer to MAC affinity to remove cationic dyes more than anionic dyes. Apparently, there was no substantial change in the adsorption efficiency among the 10 adsorption–desorption cycles. Overall, MAC can be considered as an effective and efficient viable adsorbent for cationic and anionic dyes removal from industrial wastewaters.

Key words | dye, isotherm, kinetic, magnetic activated carbon, nanocomposite, simultaneous removal

Samer Abuzerr
Amir Hossein Mahvi (corresponding author)
Department of Environmental Health Engineering,
Faculty of Public Health, International Campus,
Tehran University of Medical Sciences,
Tehran,
Iran
E-mail: *ahmahvi@yahoo.com*

Samer Abuzerr
Ministry of Health,
Gaza Strip,
Palestinian Territories

Maher Darwish
Pharmaceutical Quality Assurance Research Center, Faculty of Pharmacy, International Campus,
Tehran University of Medical Sciences,
Tehran,
Iran

Amir Hossein Mahvi
Center for Solid Waste Research, Institute for Environmental Research,
Tehran University of Medical Sciences,
Tehran,
Iran

INTRODUCTION

Nowadays, water pollution throughout the accelerated industrial activities has become the main concern, where the water effluents of textile, leather, pharmaceutical, printing, plastic, rubber, cosmetic, and food industries comprise considerable quantities of colors (Dasgupta *et al.* 2015). It is worth mentioning that 10–15% out of 700,000 tons of dyes disposed directly into the environment without sufficient treatment because of technological and economical indigence (Sivaprakasha *et al.* 2017). Organic dyes are impressively water-soluble and durable to decompose under light or oxidant agents due to their high stability originated from the synthetic origin and complex aromatic structure with many substituents that generally reinforce the stability of aromatic ring (Lu & Liu 2010; Gupta *et al.* 2013). Moreover, the majority of such dyes can pose particularly severe health risks for the human and aquatic ecosystem as a consequence of their possibility to cause carcinogenic, toxicogenic, mutagenic, and esthetical hazards (Mahvi & Heibati 2010; Tang *et al.* 2014). The dyes effect on the aquatic life lies in curtailment of photosynthetic activity of aquatic plants (Özdemir *et al.* 2006). However, cationic dyes are to cause as much harm as anionic dyes, since they have a high capacity to penetrate the cell membrane of aquatic biota facilitated by the easy interaction with negatively charged cells membrane surfaces (Li 2010; Singh *et al.* 2011).

As a matter of fact, numerous wastewater treatment methods have been employed comprised of physical, chemical, and biological processes (Assi *et al.* 2017). Notwithstanding, some of the above-mentioned processes had achieved high-efficiency water treatment field but they also had some drawbacks like being time-consuming, generating byproducts, and having a high cost (Xu *et al.* 2012). Therefore, there is a dire need to remove such pollutants from

doi: 10.2166/wst.2018.145

the industrial water effluents before reaching the natural environment in order to maintain the sustainability of the ecosystem. Adsorption process as a physico–chemical treatment method has been recognized as a promising technique for the removal of a variety of pollutants due to the lower cost, design flexibility, and operational simplicity. Furthermore, the produced water would be free of oxidation by-products that might be, in some cases, of the same or even higher toxicity than the original pollutants (Shirmardi *et al.* 2012; Stefan 2017).

Over the past few years, both natural and synthetic adsorbents have been used to treat industrial effluents, among them, for instance, were activated carbon, carbon nanotubes, clay, zeolites, graphene, polymeric resins, and modified diatomite (Adeyemo *et al.* 2012). Activated carbons (ACs) got a good reputation as effective and efficient adsorbents as a result of their unique structures, high adsorption capacity, and chemical inertness (Bhatnagar *et al.* 2013). Nevertheless, rising prices of the commercial activated carbon have motivated researchers to seek natural alternatives as low-cost adsorbents and assess their competency toward dyes removal from polluted water and so many of these low-cost bioresources adsorbents have been applied (Gupta 2009; Foo & Hameed 2012). The major shortcoming of nanoadsorbents such as activated carbon and carbon nanotubes is the difficulties in completely separating from aqueous solution by filtration and centrifugation methods because of their small size and secondary turbidity (Thinh *et al.* 2013). Remarkably, introduction of the magnetic property to the activated carbon through the combination with iron oxide nanoparticles such as Fe_3O_4 provided unique characteristics for the adsorbents to overcome obstacles regarding the separation process by collection of magnetic adsorbent from the aqueous medium easily and with high efficiency using an external magnetic field (Kakavandi *et al.* 2014; Wang *et al.* 2014). Magnetic segregation of magnetic nanoparticles from flowing industrial effluents has been broadly used and relied on (Yavuz *et al.* 2009). To that end, high gradient magnetic separation is commonly used. A magnetic field is carried out through metal wires immersed in the flowing water. To attain effective magnetic separation, a high magnetic field gradient is required that counts on the size of the magnetic particles and distance away from the magnetic field source (de Vicente *et al.* 2010; Wang *et al.* 2011). The captured magnetic nanoparticles need to be regenerated and reused for more technical feasibility in case of large-scale wastewater treatment (Gómez-Pastora *et al.* 2014). In order to regenerate the magnetic nanoparticles, methanol (MetOH) or ethanol (EtOH) are commonly used in the desorption process (Giri *et al.* 2011; Ge *et al.* 2012). Furthermore, acetic acid in methanol (HAc_{MetOH}) and HCl aqueous solutions (HCl_{aq}) and HCl ethanolic solutions (HCl_{EtOH}) also have stated high-quality desorption performance for cationic dyes (Inbaraj & Chen 2011; Ge *et al.* 2012; Zhang *et al.* 2013). Accordingly, the effluent stream of the regeneration eluent has to be treated. The main suggested handling process for desorbed dyes are: (i) reuse, (ii) incineration and (iii) solidification/stabilization processes. However, the thermal techniques are not desirable as they are too costly, not economically viable, and the probability of production of dioxins and furans is high as a result of chloride presence (Qadri *et al.* 2009; Zhang *et al.* 2013).

From this point forward, the purpose of this work was to investigate the simultaneous removal of MB as a cationic dye and RR198 as an anionic dye using magnetic activated carbon (MAC) by Fe_3O_4 as an adsorbent, to study the isotherms and kinetics of the adsorption process, and to evaluate the regenerability and reusability of the adsorbent. None of this has been studied in the literature to our knowledge.

MATERIALS AND METHODS

Materials

All materials were in analytical grade and used without any further purification. The cationic MB was purchased from Merck and the anionic mono azo RR198 dye with 95% purity was purchased from Alvan Sabet Company, Hamedan, Iran. The MAC was synthesized according to the method given by Rezaei Kalantry *et al.* (2016). The properties of MAC attained by many characterization techniques demonstrated that the morphology of MAC contained cubic Fe_3O_4 particles of less than 80 nm in diameter. Also, approximately 28% of the surface of powdered activated carbon has been occupied by iron in the form of Fe_3O_4 nanoparticles. The specific surface area of the MAC measured using Brunauer–Emmett–Teller (BET) analysis was 671.2 m^2/g with mesoporous structure. Finally, the magnetization study revealed that the highest saturation magnetization obtained for MAC was 6.94 emu/g underlying the superparamagnetic characteristic and suggesting the MAC with excellent magnetic response to magnetic field. So, this magnetic composite could be applied as an adsorbent for environmental purposes and then it could be easily and rapidly removed from the solution.

Double distilled water was used throughout the study. Hydrochloric acid (HCl) and sodium hydroxide (NaOH) were obtained from Merck, Germany. The molecular characteristics and chemical structures of the two studied dyes illustrated in Table 1.

Adsorption experiments

Adsorption studies were carried out to examine the simultaneous adsorption of both MB and RR198 dyes from aqueous solutions on the MAC as an adsorbent. Initially, the effect of pH on MAC nanoparticles absorptivity toward cationic MB, anionic RR198 dyes were tested separately for each dye, after that, the mixture was studied. Five pH values of dyes solutions were adjusted to 4, 5.5, 7, 8.5 and 10 using 0.1 M HCl or 0.1 M NaOH solutions. The effect of MAC dosages was assessed at 0.025, 0.05, and 0.1 g/100 mL. Also, the initial concentrations of the dyes were explored at 20, 40, and 60 mg/L. The dyes concentration and adsorbent dosage employed in our study are inconsistent with previous studies because the dye concentration in the textile industry effluents ranges from 0.01 g/L to 0.25 g/L relying on the type of the dye and the process carried out (Greijer *et al.* 2001; Wambuguh & Chianelli 2008). Vat dyes were found at a concentration in the range of 0.05–0.1 g/L (Ren 2000; Wambuguh & Chianelli 2008), while indigo dyes were found at a concentration of 0.02 g/L (Wambuguh & Chianelli 2008). Moreover, the dosages of activated carbon employed for direct removal dyes from spent textile dyeing wastewater were from 0.01 to 0.3 g/100 mL (Malik 2004).

The adsorption kinetics and isotherms experiments were conducted in a typical adsorption system of 100 mL dyes solution in a 250 mL sealed glass bottles under optimal conditions with 0.05 g/100 mL of MAC, the pH values for MB and RR198 solutions were 10 and 5.5, respectively, and initial dyes concentrations were 20, 40, and 60 mg/L. The adsorbent was well mixed with the dye solution at room temperature 25 °C using a shaker 150 rpm until reaching the equilibrium. When the equilibrium state was achieved at time t, the adsorbent was collected from the solution using an external magnet with dimensions 5 cm × 4 cm × 4 cm and intensity 1.3 Tesla. Each experiment was duplicated under identical conditions. Two adsorption kinetic models were implemented to evaluate the adsorption rate at three above-mentioned dyes concentrations which were pseudo-first order and pseudo-second order models. Furthermore, two classical isotherm models were inspected to identify the adsorption mechanism and obtain the theoretical maximum adsorption capacity which were Langmuir and Freundlich models.

The UV-Vis absorbency of the lowest MB concentration ($A_{(20\ mg/L)} = 0.972$ at $\lambda_{max} = 664$ nm) was well observed and not importantly affected by the adjacent RR198 peak in their mixtures. Therefore, the concentration of MB at different time intervals was determined using UV-Vis spectrophotometer (PerkinElmer UV-Vis spectrophotometer) at a maximum wavelength of 664 nm. On the other hand, the absorbency of all RR198 concentrations was very low ($A_{(20\ mg/L)} = 0.0189$ at $\lambda_{max} = 520$ nm) and there was a noteworthy interference with MB peak tail in the mixtures. Hence, the concentration of RR198 was determined using high performance liquid chromatography (HPLC) system (Knauer, Germany). The reverse-phase column used was a (C18, 5 μm 25 × 0.46). The mobile phase was a mixture of water and methanol in a ratio (50:50) adjusted at pH = 5.5, isocratically delivered by a pump at a flow rate of 1 mL/min. The wavelength of the UV absorbance detector was 254 nm.

Table 1 | General characteristics of MB and RR198 dyes

Characteristics	Methylene Blue MB	Reactive Red 198 (RR198)
Chemical structure	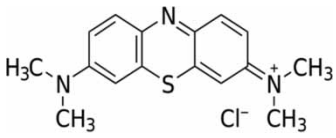	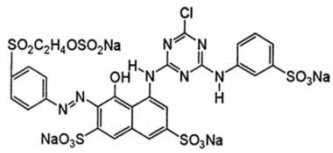
Molecular formula	$C_{16}H_{18}CHN_3.3H_2O$	$C_{27}H_{18}ClN_7Na_4O_{15}S_5$
Molecular weight	373.9 g/mol	984.183 g/mol
λ_{max}	665 nm	520 nm
Chemical class	Cationic dye	Anionic dye

The percentage of dye removal, the amount of adsorbed dye q_t (mg/g) at different time t (min), and the adsorption capacity at the equilibrium q_e (mg/g) were calculated as:

$$Dye\ removal\ \% = \frac{(C_0 - C_t)}{C_0} \times 100 \quad (1)$$

$$q_t = \frac{(C_0 - C_t)V}{W} \quad (2)$$

$$q_e = \frac{(C_0 - C_e)V}{W} \quad (3)$$

where C_0 and C_e (mg/L) are the initial liquid-phase and equilibrium concentrations of the dye, respectively. C_t (mg/L) is the liquid-phase concentration of dye at any time t. V is the volume of the dye solution (L) and W is the weight of adsorbent (g).

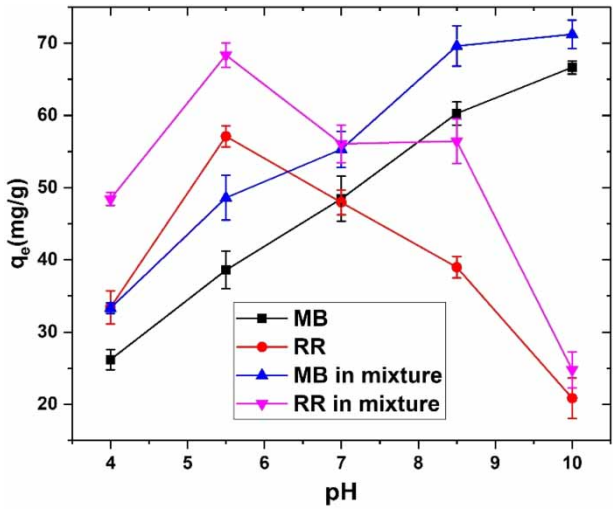

Figure 1 | Effect of initial pH on adsorption capacities of MB and RR198 in the single system individually and in a mixed solution after 120 min.

RESULTS AND DISCUSSION

Effect of pH value

The adsorption processes subject to the nature of the electrostatic reactions between the adsorbent and dye in the aqueous solutions due to the likelihood of amendments in the adsorbent active sites charges and chemistry of dye molecules (Dávila-Jiménez *et al.* 2005; Darwish *et al.* 2017). As shown in Figure 1, the adsorption capacity of cationic MB and anionic RR198 dyes was significantly affected by the pH of the solution. The initial dye concentrations were 40 mg/L for each dye and the solution volume was 100 mL at room temperature 25 °C.

The adsorption capacity for MB cationic dye in the single system individually improved drastically from 26.31 to 66.64 mg/g in tandem with increasing of pH values from 4 to 10, respectively. The increase in MB sorption at alkaline pH often relates to the dye altered surface polarity from negative to positive charge, thereby resulting in an increased uptake of cationic dye due to an increase in the electrostatic attraction between the positively charged dye and negatively charged MAC (Pathania *et al.* 2017). On the other hand, a different outcome was obtained in the case of RR198 anionic dye, the acidic medium with pH 5.5 was the favorable aqueous medium for the superior adsorption capacity 57.10 mg/g in the single system. A steady decline in the adsorption capacity above pH 5.5 was observed, indicating the high level of electrostatic repulsion between the negatively charged surface of MAC and RR198 anionic dye molecules (Xiao *et al.* 2012).

Advantageously, the coexistence of cationic MB and anionic RR198 dyes in the solution established a mutually beneficial enhancement in the adsorption capacity. The MAC adsorption capacity toward either MB or RR198 as a mixture has risen markedly across the tested pHs in comparison with signal dye systems.

The point of zero charge (pH_{pzc}) of PAC is around 5.45. At the pH_{pzc}, the surface charge is neutral and at the pH values below 5.45, the surface of PAC will be positively charged. On the other hand, it will be negatively charged at pH values above 5.45 (Üner *et al.* 2016). At low pH, we propose that positively charged MAC is able to electrostatically interact with one negative group of RR198, and the other groups can pull cationic MB. Hence, the adsorption capacity of MB increases. On the other hand, it is known that MB in solution could form dimers, trimers and higher aggregates through self-aggregation depending on the concentrations. Especially, cationic MB dimerization could be promoted in the presence of anionic dyes (Morgounova *et al.* 2013; Florence & Naorem 2014). At high pH, the MB dimer carries a positive charge at each end due to the repulsion force between them. So, one end of the dimer is linked with the negatively charged MAC, and the other end attracts an RR198 molecule (Li *et al.* 2017). Consequently, an elevation of the adsorption capacity of both RR198 and MB is observed in the mixture solution across the tested pH range.

Effect of contact time and initial concentration of dyes

Three initial dyes concentrations were studied: 20, 40, and 60 mg/L under the optimal conditions with 0.05 g/100 mL of MAC, 100 mL of dyes solution, and the pH values for MB and RR198 individual and mixed solutions were 10 and 5.5, respectively.

As illustrated in Figure 2, the adsorption capacity for both MB and RR198 dyes in the mixture increased from 37.75 to 101.47 mg/g and from 36.43 to 93.69 mg/g, respectively, with a corresponding increase in initial concentration from 20 to 60 mg/L. The positive association between the adsorption capacity and initial dye concentration owing mostly to improvements in the driving force of diffusion. Increased number of dye molecules means increasing the number of collisions of dye molecules with adsorbent surface that tend to enforce more mass transfer from solution phase to solid phase (Ip *et al.* 2010).

Also from Figure 2, the adsorption process of MB and RR198 dyes onto MAC principally comprised three phases: during the first 30 min, the rapid increase in the dyes adsorption indicates the uptake rate to be fast toward both anionic and cationic dyes. This logical consequence can be explained as a strong driving force of the concentration gradient between the adsorbate and adsorbent due to the high availability of unoccupied sites on the adsorbent surface in the initial phase. From 30–90 min, the equilibrium adsorption capacity gradually slowed down over time as the dye molecules diffused into the adsorbent pores through the intra-particle mass transfer process and accumulate in the active sites, so, the sorption rate was down from the last phase and eventually reached the equilibrium in the third phase after 120 min due to low solute concentration in the solution (Alkan *et al.* 2008).

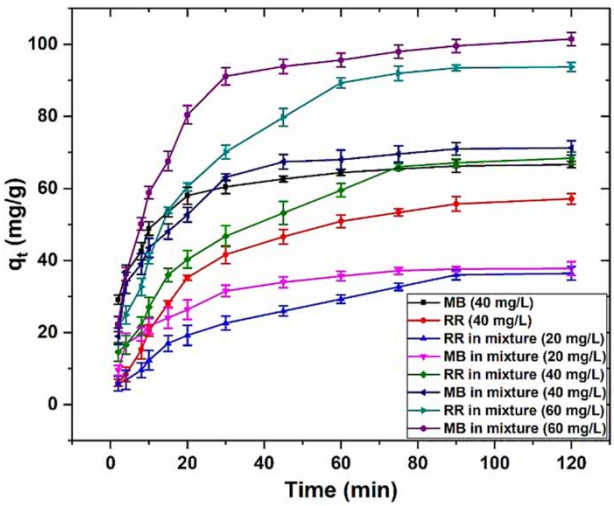

Figure 2 | Effect of contact time and initial concentration of dyes on the adsorption capacity of MB and RR198 dye on MAC.

Furthermore, it was observed that the contact time needed for the MB and RR198 solutions to reach equilibrium was around 120 min regardless of the initial concentration used. This result might be an indicator that the intraparticle diffusion is not the only rate limiting mechanism in the adsorption process. Some other mechanisms along with intraparticle diffusion are also involved such as surface adsorption that might simultaneously occur with intraparticle diffusion during the MB, RR198 and MAC interactions (Xue *et al.* 2013). Consequently, 120 min has been considered as equilibrium time and further experiments were conducted at 120 min.

Effect of MAC dosage and the initial dyes concentrations

Three MAC dosages were examined: 0.025, 0.05, and 0.1 g/100 mL on three dye concentrations: 20, 40, and 60 mg/L under the optimal conditions of 100 mL of dyes solution, time of 120 min, and the pH values for MB and RR198 solutions were 10 and 5.5, respectively. As reflected in Figure 3, as a corollary to increase adsorption surface area (Cechinel & de Souza 2014), the adsorption efficiency of MAC toward MB in the mixture solution increased from 88.6 to 96.9%, 83.4 to 92.2%, and 75.3 to 86.1% at initial dye concentrations from 20 to 60 mg/L and MAC dosages from 0.025 to 0.1 g/100 mL, respectively. Also, with the same pattern, the adsorption efficiency of MAC toward RR198 was raised from 84.8 to 93.7%, 80.1 to 87.9%, and 71.4 to 80.2% at initial dye concentrations from 20 to 60 mg/L and MAC dosages from 0.025 to 0.1 g/100 mL, respectively, as a corollary to increasing adsorption surface area. It is worth emphasizing that there was not much difference in the removal efficiency between the two MAC dosages 0.05 and 0.1 g/100 mL when the dyes concentrations were 40 mg/L. Therefore, 0.05 g/100 mL of MAC dosage was considered as an optimal amount. Moreover, the shortfall in the adsorption efficiency with the rise in the dye concentration from 20 to 60 mg/L basically ascribes to increase the number of dye molecules in higher concentration, as well as only a limited number of active sites being available on the adsorbent surface (Ghaedi *et al.* 2012).

Adsorption kinetic models

To understand the mechanism of simultaneous adsorption process and to determine the effect of influential factors

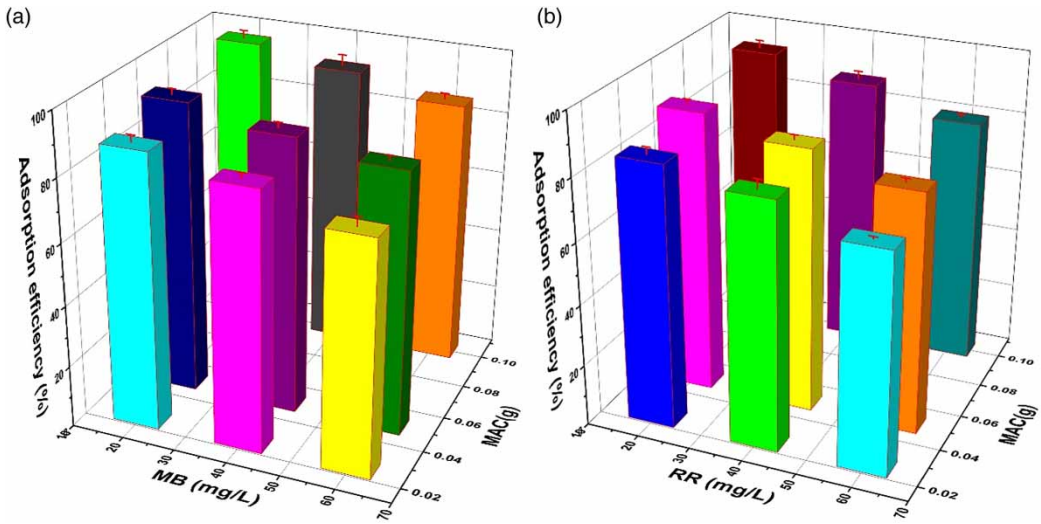

Figure 3 | Effect of MAC dosage and different initial concentrations of dyes on the adsorption efficiency of (a) MB and (b) RR198 dyes on MAC.

on the reaction rate, the adsorption kinetics must be examined. As was explained above and presented in Figure 4(a) and 4(b), the adsorption capacity was calculated at different time intervals t during the adsorption process in accordance with the best parameters for each dye using three concentrations of dye: 20, 40, and 60 mg/L. Two kinetic models, pseudo-first order, and pseudo-second order were employed in this work to explore the kinetic process of MB and RR198 adsorption onto MAC nanoparticles. Based on the pseudo-first order rate equation (Ho & McKay 1998), the adsorption rate is depending on the adsorption capacity; the linear equation in logarithms is as follows:

$$\ln(q_e - q_t) = \ln q_e - k_1 t \tag{4}$$

where q_t is the amounts of dye adsorbed by adsorbent (mg/g) at time t (min); k_1 is the pseudo-first order rate constant (min^{-1}). Also, the pseudo-second order kinetic is checked as a chemisorption mechanism through sharing or exchanging the electrons between the dyes and MAC. The linear second-order equation is expressed as follows (El-Khaiary *et al.* 2010):

$$\frac{t}{q_t} = \frac{1}{k_2 q_e^2} + \frac{t}{q_e} \tag{5}$$

where k_2 is the pseudo-second order rate constant (g/mg·min).

Table 2 shows the values of kinetic parameters of MB and RR198 adsorption on MAC. It can be seen that pseudo-first order model owned lower correlation coefficients (R^2) for MB and RR198 at all concentrations as compared with the pseudo-second order with (R^2) values close to unity (>0.98) (Figure 4(c)–4(f)). Furthermore, pseudo-first order model anticipated much lower values of q_e than the experimental ones, making this model inappropriate to describe MB adsorption. However, in the case of RR198, the values were fairly close. On the other hand, the experimental and calculated values of q_e from the pseudo-second order model were adequately approximate in all cases for both dyes. The main assumptions for these findings are that the adsorption fits well to the pseudo-second order kinetic and the overall rate of MB and RR198 adsorption process is controlled by chemisorption. The rate-limiting step is presumably the chemical interactions involving electrostatic forces through the exchange of electrons between MB, RR198, and MAC (Dhorabe *et al.* 2016).

Adsorption isotherm models

In the present study, the obtained outcomes from the equilibrium experiments of MB and RR198 simultaneous adsorption by MAC were analyzed using the well-known isotherm models, Langmuir and Freundlich, to understand the distribution of the adsorption molecules on solid phase at the equilibrium condition. The main differences between Langmuir and Freundlich adsorption models are that Langmuir assumes a monolayer of adsorbate molecules covers the adsorbent surface homogenously, while in Freundlich, heterogeneously by monolayer adsorption (Wu *et al.* 2012;

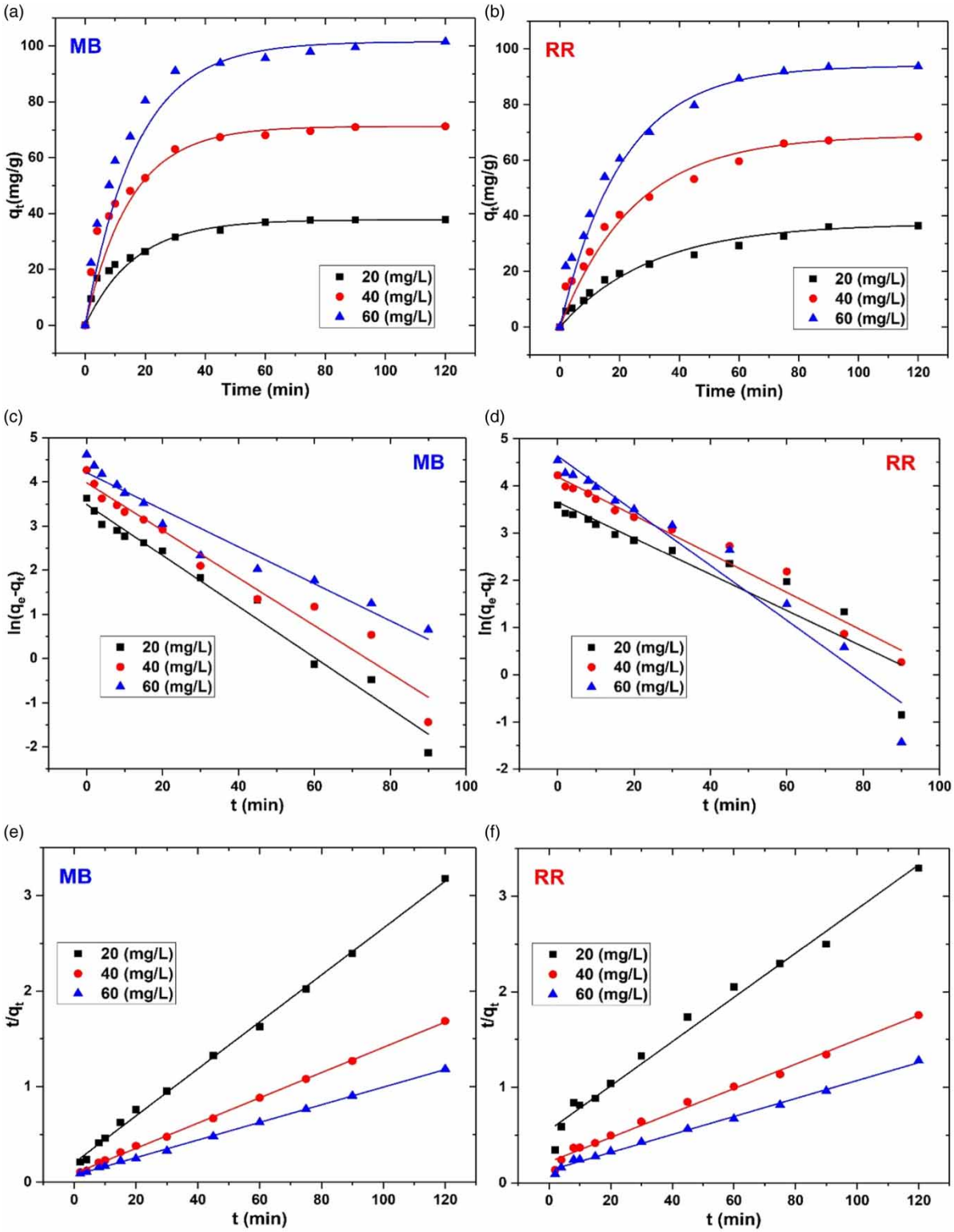

Figure 4 | Adsorption capacity of (a) MB and (b) RR198 as a function of time at different initial concentrations; linear regressions of (c) MB and (d) RR98 according to pseudo-first order kinetic model; linear regressions of (e) MB and (f) RR198 according to pseudo-second order kinetic model.

Table 2 | The first- and second-order kinetics models for adsorption of MB and RR198 dyes on the MAC at 25 °C

			Kinetic models					
			Pseudo-first order			Pseudo-second order		
Dye	Con. (mg/L)	Exp. q_e (mg/g)	K_1 (min^{-1})	Calc. q_e (mg/g)	R^2	K_2 (g/mg min)	Calc. q_e (mg/g)	R^2
MB	20	37.75	0.0578	32.82	0.982	0.003	40.65	0.998
	40	71.23	0.054	53.57	0.965	0.0019	75.75	0.999
	60	101.5	0.042	67.36	0.952	0.0012	108.7	0.999
RR198	20	36.43	0.0384	38.7	0.881	1×10^{-3}	43.29	0.985
	40	68.36	0.0409	66.15	0.971	7×10^{-6}	78.12	0.992
	60	93.69	0.0581	102.72	0.959	7×10^{-4}	106.38	0.995

Purevsuren *et al.* 2015). Another difference is that in Langmuir, a chemical reaction happens between the adsorbate molecules and free sites, while in Freundlich, physical reaction occurs (Lin *et al.* 2011).

It must be noted that these assumptions were originally developed for gas adsorption on solid surface. In liquid–solid systems, with the hydration forces, mass transport effects, etc., the system is much more dynamic and complicated, and obeying the isotherm does not necessarily reflect the validity of the aforementioned assumptions. In such systems, the isotherm adequacy can be seriously affected by the experimental conditions; in particular, the range of concentration of the solute/adsorbate. Both Langmuir and Freundlich isotherms might adequately describe the same set of liquid–solid adsorption data at certain concentration ranges, in particular if the concentration is small and the adsorption capacity of the solid is large enough to make both isotherm equations approach a linear form.

The linear form of the Langmuir and Freundlich isotherms is represented by the following equations, respectively:

$$\frac{C_e}{q_e} = \frac{1}{q_m K_L} + \frac{1}{q_m} C_e \tag{6}$$

$$\ln q_e = \ln K_F + \frac{1}{n} ln\ C_e \tag{7}$$

where C_e (mg/L) is the equilibrium dye concentration in solution, q_m (mg/g) is the maximum capacity of the adsorbent, and K_L (L/mg), the Langmuir constant, K_F is a Freundlich constant and n is the heterogeneity factor related to the capacity and intensity of adsorption, respectively.

Table 3 and Figure 5 summarize the results of fitting with the two selected isotherm models parameters and their linearity which applied at three initial dyes concentrations 20, 40, 60, 80 and 100 mg/L, MAC dosage of 0.05 g/100 mL, fixed pH 10 for MB and pH 5.5 for RR198, and at a room temperature of 25 °C. Based on high linear correlation coefficient R^2 values, the results revealed that adsorption of MB on the MAC had the best-fitting with Freundlich model ($R^2 = 0.999$) (Figure 6(b)), also Langmuir was acceptable ($R^2 = 0.979$) (Figure 6(a)). Whereas RR198 adsorption on the MAC shows more validity by Langmuir ($R^2 = 0.999$) as in Figure 5(c) than Freundlich ($R^2 = 0.981$) (Figure 5(d)). The very good correlation between experimental data and Langmuir isotherm model at different concentrations of the solution imply the uniform distribution of homogeneous active sites on the adsorbent surface (Chowdhury & Yanful 2011). This result, consistent with other previous research, mentioned that the Langmuir isotherm was the best model for the adsorption of reactive dyes on activated carbon as well (Senthilkumaar *et al.* 2006; Ahmad & Rahman 2011; Xiao *et al.* 2012). Furthermore, the higher value of Freundlich adsorption capacity (K_f) for MB in comparison with RR198 refer to MAC affinity to remove cationic dyes more than anionic dyes. In conclusion, the most appropriate isotherms for simultaneous adsorption system of MB and RR198 on MAC were Freundlich and Langmuir models, respectively. The cooperative adsorption of MB and RR198 suggests that we may have found a system that can fairly be called multilayer adsorption.

Table 3 | Isotherm parameters of MB and RR198 adsorption onto MAC

Isotherm model	Langmuir			Freundlich		
Dye	q_m (mg/g)	K_L (L/mg)	R^2	$K_F^{1/n}$ ($_{mg/g(L/mg)}$)	*n*	R^2
MB	169.49	0.193	0.979	35.85	2.16	0.999
RR198	129.87	0.204	0.999	30.05	2.36	0.981

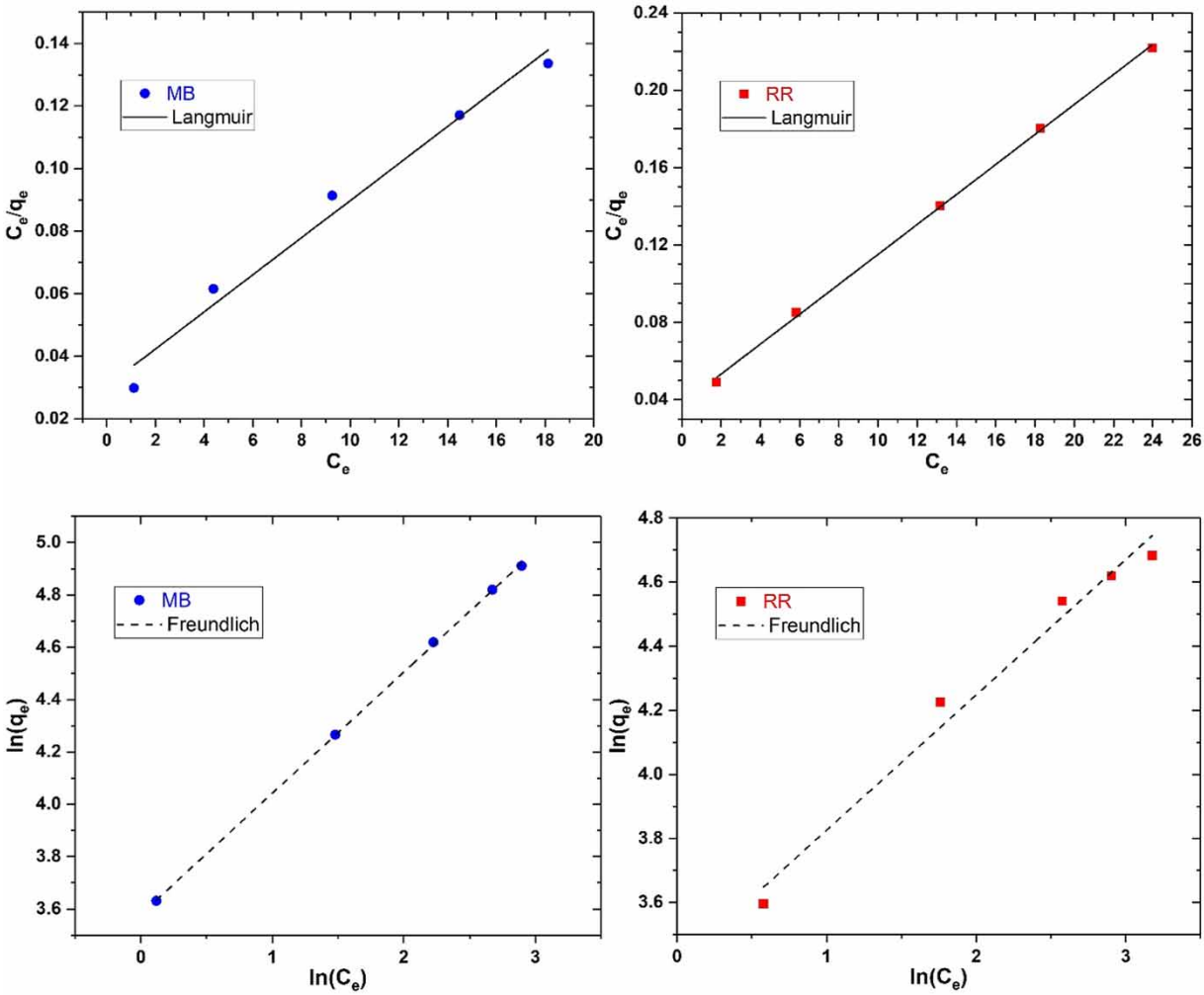

Figure 5 | Langmuir model of (a) MB and (b) RR198 adsorption onto MAC. Freundlich model of (c) MB and (d) RR198 at five different initial concentrations.

The reusability of MAC

The ease of magnetic adsorbents regeneration is an exclusive and economically and environmentally friendly feature. Figure 6 presents ten adsorption cycles were applied in order to inspect the removal proficiency of MAC toward cationic and anionic dyes over ten adsorption and desorption cycles under the above-described optimum conditions. As already mentioned in the methodology section, after attaining the adsorption equilibrium, the external magnet was used to separate the MAC from the aqueous solution, then spectrophotometer and HPLC were used for MB and RR198 analysis, respectively. The desorption process was performed in a 250 mL glass bottle with 0.1 g of MAC loaded with MB and RR198 dyes; subsequently, 10 mL of 0.1 M

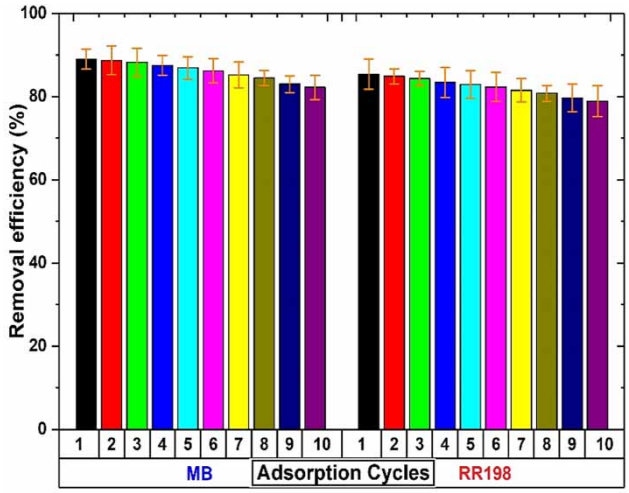

Figure 6 | Ten adsorption cycles of MAC towards removal of MB and RR198 dyes.

HCl/methanol (1:9, v/v) was added as a desorbing solution. The solution shacked at room temperature 25 °C using a shaker 150 rpm for 120 min. The 0.1 M HCl/methanol (1:9, v/v) was adopted as desorption solution in order to avoid altering the MAC morphology and physical characteristics.

Apparently, there was no substantial change in the adsorption efficiency among the ten adsorption–desorption cycles. The adsorption percentage of MB and RR198 dyes on MAC decreased from 89 to 82.2% and from 85.46 to 78.9%, respectively, after ten reuse cycles. The reason behind the high desorption level is likely as a result of protonation of the adsorbent surface with the acidic agent. Noting with interest, MAC can be considered as an effective and efficient viable adsorbent for cationic and anionic dyes removal from industrial wastewaters.

CONCLUSION

MAC nanoparticles were prepared in order to investigate their simultaneous adsorption of cationic dye (MB) and anionic dye (RR198) from aqueous solution. The effect of solution pH, contact time, adsorbent amount, and dye concentration were studied. Also, both kinetic and isotherm experiments were achieved. The optimum pH was 10 and 5.5 for adsorption of MB and RR198, respectively, and the equilibrium status was achieved after 120 min. The adsorption kinetics was controlled by the pseudo-second order kinetic model more than pseudo-first order. The best-fitted isotherms were Freundlich and Langmuir models MB and RR198, respectively. The higher value of Freundlich adsorption capacity (K_f) for MB in comparison with RR198 refer to MAC affinity to remove cationic dyes more than anionic dyes. Apparently, there was no substantial change in the adsorption efficiency among the ten adsorption–desorption cycles.

Overall, MAC can be considered as an effective and efficient viable adsorbent for cationic and anionic dyes removal from industrial wastewaters. However, in order to mitigate the effects of suspended solids and the pH effect on the adsorption rate and adsorption capacity, adsorption processes might as well to be applied for biologically treated sewage effluents in terms of the presence of low suspended solids concentration levels and more favorable chemical composition of the sewage effluent organics, since acid and alkaline pH regions are preferred to the neutral pH region.

ACKNOWLEDGEMENTS

Authors would like to thank the laboratories team at Environmental Health Engineering Department, Tehran University of Medical Sciences, International campus for their materials and instrumental support. Also, we would like to express our gratitude for Eng. Shahrokh Nazmara, Eng. Sara Hosseini and Eng. Babak Mahmoudi for their technical assistance.

REFERENCES

Adeyemo, A. A., Adeoye, I. O. & Bello, O. S. 2012 Metal organic frameworks as adsorbents for dye adsorption: overview, prospects and future challenges. *Toxicological & Environmental Chemistry* **94** (10), 1846–1863.

Ahmad, M. A. & Rahman, N. K. 2011 Equilibrium, kinetics and thermodynamic of Remazol Brilliant Orange 3R dye adsorption on coffee husk-based activated carbon. *Chemical Engineering Journal* **170** (1), 154–161.

Alkan, M., Doğan, M., Turhan, Y., Demirbaş, Ö. & Turan, P. 2008 Adsorption kinetics and mechanism of maxilon blue 5G dye on sepiolite from aqueous solutions. *Chemical Engineering Journal* **139** (2), 213–223.

Assi, N., Aberoomand Azar, P., Saber Tehrani, M., Waqif Husain, S., Darwish, M. & Pourmand, S. 2017 Synthesis of ZnO-nanoparticles by microwave assisted sol-gel method and its role in photocatalytic degradation of food dye Tartrazine (Acid Yellow 23). *International Journal of Nano Dimension* **8** (3), 241–249.

Bhatnagar, A., Hogland, W., Marques, M. & Sillanpää, M. 2013 An overview of the modification methods of activated carbon for its water treatment applications. *Chemical Engineering Journal* **219**, 499–511.

Cechinel, M. A. P. & de Souza, A. A. U. 2014 Study of lead (II) adsorption onto activated carbon originating from cow bone. *Journal of Cleaner Production* **65**, 342–349.

Chowdhury, S. R. & Yanful, E. K. 2011 Arsenic removal from aqueous solutions by adsorption on magnetite nanoparticles. *Water and Environment Journal* **25** (3), 429–437.

Darwish, M., Mohammadi, A. & Assi, N. 2017 Partially decomposed PVP as a surface modification of ZnO, CdO, ZnS and CdS nanostructures for enhanced stability and catalytic activity towards sulphamethoxazole degradation. *Bulletin of Materials Science* **40** (3), 513–522.

Dasgupta, J., Sikder, J., Chakraborty, S., Curcio, S. & Drioli, E. 2015 Remediation of textile effluents by membrane based treatment techniques: a state of the art review. *Journal of Environmental Management* **147**, 55–72.

Dávila-Jiménez, M., Elizalde-González, M. & Peláez-Cid, A. 2005 Adsorption interaction between natural adsorbents and textile dyes in aqueous solution. *Colloids and Surfaces A: Physicochemical and Engineering Aspects* **254** (1), 107–114.

de Vicente, I., Merino-Martos, A., Cruz-Pizarro, L. & de Vicente, J. 2010 On the use of magnetic nano and microparticles for lake restoration. *Journal of Hazardous Materials* **181** (1), 375–381.

Dhorabe, P. T., Lataye, D. H. & Ingole, R. S. 2016 Removal of 4-nitrophenol from aqueous solution by adsorption onto activated carbon prepared from *Acacia glauca* sawdust. *Water Science and Technology* **73** (4), 955–966.

El-Khaiary, M. I., Malash, G. F. & Ho, Y.-S. 2010 On the use of linearized pseudo-second-order kinetic equations for modeling adsorption systems. *Desalination* **257** (1), 93–101.

Florence, N. & Naorem, H. 2014 Dimerization of methylene blue in aqueous and mixed aqueous organic solvent: a spectroscopic study. *Journal of Molecular Liquids* **198** (Supplement C), 255–258.

Foo, K. & Hameed, B. 2012 Factors affecting the carbon yield and adsorption capability of the mangosteen peel activated carbon prepared by microwave assisted K_2CO_3 activation. *Chemical Engineering Journal* **180**, 66–74.

Ge, F., Ye, H., Li, M.-M. & Zhao, B.-X. 2012 Efficient removal of cationic dyes from aqueous solution by polymer-modified magnetic nanoparticles. *Chemical Engineering Journal* **198**, 11–17.

Ghaedi, M., Sadeghian, B., Pebdani, A. A., Sahraei, R., Daneshfar, A. & Duran, C. 2012 Kinetics, thermodynamics and equilibrium evaluation of direct yellow 12 removal by adsorption onto silver nanoparticles loaded activated carbon. *Chemical Engineering Journal* **187**, 133–141.

Giri, S., Das, N. & Pradhan, G. 2011 Synthesis and characterization of magnetite nanoparticles using waste iron ore tailings for adsorptive removal of dyes from aqueous solution. *Colloids and Surfaces A: Physicochemical and Engineering Aspects* **389** (1), 43–49.

Gómez-Pastora, J., Bringas, E. & Ortiz, I. 2014 Recent progress and future challenges on the use of high performance magnetic nano-adsorbents in environmental applications. *Chemical Engineering Journal* **256**, 187–204.

Greijer, H., Karlson, L., Lindquist, S.-E. & Hagfeldt, A. 2001 Environmental aspects of electricity generation from a nanocrystalline dye sensitized solar cell system. *Renewable Energy* **23** (1), 27–39.

Gupta, V. 2009 Application of low-cost adsorbents for dye removal–a review. *Journal of Environmental Management* **90** (8), 2313–2342.

Gupta, V. K., Kumar, R., Nayak, A., Saleh, T. A. & Barakat, M. A. 2013 Adsorptive removal of dyes from aqueous solution onto carbon nanotubes: a review. *Advances in Colloid and Interface Science* **193–194** (Supplement C), 24–34.

Ho, Y. & McKay, G. 1998 A comparison of chemisorption kinetic models applied to pollutant removal on various sorbents. *Process Safety and Environmental Protection* **76** (4), 332–340.

Inbaraj, B. S. & Chen, B. 2011 Dye adsorption characteristics of magnetite nanoparticles coated with a biopolymer poly (γ-glutamic acid). *Bioresource Technology* **102** (19), 8868–8876.

Ip, A. W., Barford, J. P. & McKay, G. 2010 A comparative study on the kinetics and mechanisms of removal of Reactive Black 5 by adsorption onto activated carbons and bone char. *Chemical Engineering Journal* **157** (2), 434–42.

Kakavandi, B., Kalantary, R. R., Farzadkia, M., Mahvi, A. H., Esrafili, A., Azari, A., Yari, A. R. & Javid, A. B. 2014 Enhanced chromium (VI) removal using activated carbon modified by zero valent iron and silver bimetallic nanoparticles. *Journal of Environmental Health Science and Engineering* **12** (1), 115.

Li, S. 2010 Removal of crystal violet from aqueous solution by sorption into semi-interpenetrated networks hydrogels constituted of poly(acrylic acid-acrylamide-methacrylate) and amylose. *Bioresource Technology* **101** (7), 2197–2202.

Li, H., Cao, X., Zhang, C., Yu, Q., Zhao, Z., Niu, X., Sun, X., Liu, Y., Ma, L. & Li, Z. 2017 Enhanced adsorptive removal of anionic and cationic dyes from single or mixed dye solutions using MOF PCN-222. *RSC Advances* **7** (27), 16273– 16281.

Lin, Y.-F., Chen, H.-W., Chien, P.-S., Chiou, C.-S. & Liu, C.-C. 2011 Application of bifunctional magnetic adsorbent to adsorb metal cations and anionic dyes in aqueous solution. *Journal of Hazardous Materials* **185** (2), 1124–1130.

Lu, X. & Liu, R. 2010 Treatment of Azo dye-containing wastewater using integrated processes. In: *Biodegradation of Azo Dyes* (H. Atacag Erkurt, ed.). Springer, Berlin and Heidelberg, Germany, pp. 133–155.

Mahvi, A. & Heibati, B. 2010 Removal efficiency of azo dyes from textile effluent using activated carbon made from walnut wood and determination of isotherms of acid red 18. *Journal of Health* **1** (3), 7–15.

Malik, P. K. 2004 Dye removal from wastewater using activated carbon developed from sawdust: adsorption equilibrium and kinetics. *Journal of Hazardous Materials* **113** (1), 81–88.

Morgounova, E., Shao, Q., Hackel, B. J., Thomas, D. D. & Ashkenazi, S. 2013 Photoacoustic lifetime contrast between methylene blue monomers and self-quenched dimers as a model for dual-labeled activatable probes. *Journal of Biomedical Optics* 18 (5), 56004.

Özdemir, Y., Doğan, M. & Alkan, M. 2006 Adsorption of cationic dyes from aqueous solutions by sepiolite. *Microporous and Mesoporous Materials* **96** (1), 419–427.

Pathania, D., Sharma, S. & Singh, P. 2017 Removal of methylene blue by adsorption onto activated carbon developed from Ficus carica bast. *Arabian Journal of Chemistry* **10** (Supplement 1), S1445–S1S51.

Purevsuren, B., Lin, C.-J., Davaajav, Y., Ariunaa, A., Batbileg, S., Avid, B., Jargalmaa, S., Huang, Y. & Liou, S. Y.-H. 2015 Adsorption isotherms and kinetics of activated carbons produced from coals of different ranks. *Water Science and Technology* **71** (8), 1189–1195.

Qadri, S., Ganoe, A. & Haik, Y. 2009 Removal and recovery of acridine orange from solutions by use of magnetic nanoparticles. *Journal of Hazardous Materials* **169** (1), 318–323.

Ren, X. 2000 Development of environmental performance indicators for textile process and product. *Journal of Cleaner Production* **8** (6), 473–481.

Rezaei Kalantry, R., Jonidi Jafari, A., Esrafili, A., Kakavandi, B., Gholizadeh, A. & Azari, A. 2016 Optimization and evaluation of reactive dye adsorption on magnetic composite of activated carbon and iron oxide. *Desalination and Water Treatment* **57** (14), 6411–6422.

Senthilkumaar, S., Kalaamani, P., Porkodi, K., Varadarajan, P. & Subburaam, C. 2006 Adsorption of dissolved reactive red dye from aqueous phase onto activated carbon prepared from agricultural waste. *Bioresource Technology* **97** (14), 1618–1625.

Shirmardi, M., Mesdaghinia, A., Mahvi, A. H., Nasseri, S. & Nabizadeh, R. 2012 Kinetics and equilibrium studies on adsorption of acid red 18 (Azo-Dye) using multiwall carbon nanotubes (MWCNTs) from aqueous solution. *Journal of Chemistry* **9** (4), 2371–2383.

Singh, K. P., Gupta, S., Singh, A. K. & Sinha, S. 2011 Optimizing adsorption of crystal violet dye from water by magnetic nanocomposite using response surface modeling approach. *Journal of Hazardous Materials* **186** (2), 1462–1473.

Sivaprakasha, S., Kumarb, P. S. & Krishnac, S. 2017 Adsorption study of various dyes on Activated Carbon Fe_3O_4 Magnetic Nano Composite. *International Journal of Applied Chemistry* **13** (2), 255–266.

Stefan, M. I. 2017 *Advanced Oxidation Processes for Water Treatment: Fundamentals and Applications*. IWA Publishing, London, UK.

Tang, L., Cai, Y., Yang, G., Liu, Y., Zeng, G., Zhou, Y., Li, S., Wang, J., Zhang, S. & Fang, Y. 2014 Cobalt nanoparticles-embedded magnetic ordered mesoporous carbon for highly effective adsorption of rhodamine B. *Applied Surface Science* **314**, 746–753.

Thinh, N. N., Hanh, P. T. B., Hoang, T. V., Hoang, V. D., Dang, L. H., Van Khoi, N. & Dai Lam, T. 2013 Magnetic chitosan nanoparticles for removal of Cr (VI) from aqueous solution. *Materials Science and Engineering: C* **33** (3), 1214–1218.

Üner, O., Geçgel, Ü. & Bayrak, Y. 2016 Adsorption of methylene blue by an efficient activated carbon prepared from Citrullus lanatus rind: kinetic, isotherm, thermodynamic, and mechanism analysis. *Water, Air, & Soil Pollution* **227** (7), 247.

Wambuguh, D. & Chianelli, R. R. 2008 Indigo dye waste recovery from blue denim textile effluent: a by-product synergy approach. *New Journal of Chemistry* **32** (12), 2189–2194.

Wang, Q., Guan, Y., Ren, X., Cha, G. & Yang, M. 2011 Rapid extraction of low concentration heavy metal ions by magnetic fluids in high gradient magnetic separator. *Separation and Purification Technology* **82**, 185–189.

Wang, N., Zhou, L., Guo, J., Ye, Q., Lin, J.-M. & Yuan, J. 2014 Adsorption of environmental pollutants using magnetic hybrid nanoparticles modified with β-cyclodextrin. *Applied Surface Science* **305**, 267–273.

Wu, X.-W., Ma, H.-W., Yang, J., Wang, F.-J. & Li, Z.-H. 2012 Adsorption of Pb (II) from aqueous solution by a poly-elemental mesoporous adsorbent. *Applied Surface Science* **258** (14), 5516–5521.

Xiao, H., Peng, H., Deng, S., Yang, X., Zhang, Y. & Li, Y. 2012 Preparation of activated carbon from edible fungi residue by microwave assisted K_2CO_3 activation – application in reactive black 5 adsorption from aqueous solution. *Bioresource Technology* **111**, 127–133.

Xu, P., Zeng, G. M., Huang, D. L., Feng, C. L., Hu, S., Zhao, M. H., Lai, C., Wei, Z., Huang, C. & Xie, G. X. 2012 Use of iron oxide nanomaterials in wastewater treatment: a review. *Science of the Total Environment* **424**, 1–10.

Xue, G., Gao, M., Gu, Z., Luo, Z. & Hu, Z. 2013 The removal of p-nitrophenol from aqueous solutions by adsorption using gemini surfactants modified montmorillonites. *Chemical Engineering Journal* **218** (Supplement C), 223–231.

Yavuz, C. T., Prakash, A., Mayo, J. & Colvin, V. L. 2009 Magnetic separations: from steel plants to biotechnology. *Chemical Engineering Science* **64** (10), 2510–2521.

Zhang, X., Zhang, P., Wu, Z., Zhang, L., Zeng, G. & Zhou, C. 2013 Adsorption of methylene blue onto humic acid-coated Fe_3O_4 nanoparticles. *Colloids and Surfaces A: Physicochemical and Engineering Aspects* **435**, 85–90.

First received 18 October 2017; accepted in revised form 18 March 2018. Available online 4 April 2018